

Investigation of the insulator to half-metal transition in Cr-doped ZnO at low temperature (19 K) wurtzite structure

Sarajit Biswas*

Dept. of Physics, Taki Government College, P.O.-Taki, Dist., North 24 Parganas, 743429, West Bengal, India

*Corresponding: srisabuj.phys@gmail.com

Abstract

The structural, electronic and magnetic properties of pure and Cr-doped ZnO with a low temperature (19 K) wurtzite structure were studied by employing density functional theory (DFT) as implemented in the tight-binding linearized-muffin-tin orbital (TB-LMTO) method. Pure ZnO is observed as a nonmagnetic insulator in which all the Zn-3d orbitals are found occupied and electrons are perfectly paired in each orbital causing nonmagnetic nature of pure ZnO. But Cr-doping in ZnO significantly changes its electronic and magnetic properties. This material encounters nonmagnetic insulator to a ferromagnetic half-metal with minute structural distortions at 50% Cr substitution for Zn. This study revealed that the doped material $Zn_{0.5}Cr_{0.5}O$ is metallic for the majority spin species and insulating for the minority spin species with a semiconducting gap of 3.5 eV. Due to the influence of the strong electron correlation effect, three Cr- t_{2g} orbitals become fully occupied by three Cr-3d electrons, while remaining single electron is shared by two e_g orbitals in the close vicinity of the Fermi level. This sharing of the single electron by two e_g orbitals is responsible for the metallic behavior of $Zn_{0.5}Cr_{0.5}O$ for the spin majority channel. The parallel alignment of unpaired electrons in the Cr-3d orbitals is responsible for the ferromagnetism of this material.

Keywords: Density functional theory (DFT); Ferromagnetism, Half-metal; Local spin density approximation (LSDA); Wurtzite structure

1. Introduction

Recently, research studies have investigated the area of wide band gap semiconductor materials due to their wide range of applications. Among them, zinc oxide (ZnO) as a II-VI compound semiconductor material has many unique features. These include its wide band gap (3.32 eV), large excitation energy (~ 60 meV), high melting point, high-temperature resistance, etc. ZnO is a promising semiconductor materials for its widespread industrial and scientific applications, such as in piezoelectric nanogenerators, transparent electrodes, ultraviolet (UV) detectors, gas sensors, optoelectronic devices, photocatalytic activity (Gao *et al.*, 2005; Battaglia *et al.*, 2011; Chai *et al.*, 2009; Yi *et al.*, 2011; Djurisi *et al.*, 2010). Many experiments have demonstrated that doping in ZnO nanoparticles influences their physical, chemical, and structural properties (Rasouli & Moeen, 2011). In order to achieve expected properties, different kinds of elements have been doped into the ZnO lattice, including rare earth elements and metals (Chen *et al.*, 2010; Gao *et al.*, 2006; Zheng *et al.*, 2011). The prime object of doping elements into ZnO nanocrystals is to increase or decrease the band gap energy of this system through the doping of exact doping elements. When doping with transition metals such as V, Cr, Fe, Co or Ni, ZnO nanoparticles turn into a promising host semiconductor

material. Dietl *et al.*, (2000) theoretically demonstrated that Mn-doped ZnO would be ferromagnetic at room temperature and could be applied to spintronic devices. In addition, other research has been carried out to improve the structural, optical and magnetic properties of Cr-doped ZnO thin films (Yilmaz *et al.*, 2011; Lin *et al.*, 2012; Iqbal *et al.*, 2013; Shah *et al.*, 2014).

In their ab initio calculations, Sato *et al.*, (2002) reported that V, Fe, Cr, Co and Ni doping in ZnO shows ferromagnetic ordering above room temperature. However, experimental studies of Cr-doping in ZnO show conflicting results. In some studies, the magnetic behavior of Cr-doped ZnO appears to be very sensitive to the deposition method. For example, Ueda *et al.* (2001) did not detect ferromagnetism in Cr-doped ZnO films synthesized by the pulse laser deposition method. However, Roberts *et al.*, (2005) detected ferromagnetic ordering at a doping concentration of 9.5% in the magnetron sputtering method. Additionally, Jin *et al.* (2001) confirmed no ferromagnetic behavior for a Cr-doped ZnO thin film at low temperature (LT) even down to 3 K. In some studies (Thota *et al.*, 2006; Bhargava *et al.*, 2011; Gad *et al.*, 2015), it was observed that for a low Cr-concentration (up to $x=0.10$), $Zn_{1-x}Cr_xO$ has a single phase, but a higher Cr-concentration ($x \geq 0.15$) confirms a secondary phase of $ZnCr_2O_4$, which gives the oxidation state of Cr as +3. Coexistence of these

two phases results in a crystal defect due to the non-homogeneous distribution of Cr into ZnO. However, Xu *et al.*, (2008) and Zhuge *et al.*, (2009) incorporated Cr in the ZnO materials uniformly and observed no secondary phase. For doping in the compound $Zn_{1-x}M_xO$ (0.05-0.25): $M=Cr, Mn, Co, Ni$, the doping level was as high as 25%, but no additional secondary phase was observed (Ueda *et al.*, 2001). It's important to note that all the cited works were carried out in the room temperature phase.

Current research is limited considering the Cr-doping effect in ZnO at low temperature (LT) structure. (Jin *et al.*, 2001; Kim *et al.*, 2014). In a study by Ueda *et al.* (2001), a doping level in the compound $Zn_{1-x}M_xO$ ($M=Cr, Mn, Co, Ni$) reached 25%. S. Thota *et al.*, (2006) reported the highest doping of 30% in ZnO by Ni, Co, Mn. Zhuge *et al.*, (2010) increased the Co-doping in ZnO up to 37.7%. Furthermore, in materials such as CrO_2 , high doping of Ru (~50%) was carried out by West *et al.*, (2015). This research showed significant changes in the electrical and magnetic properties. In addition, a higher concentration of Cr in ZnO (as much as 50%) has interestingly exhibited an insulator to half-metal transition concomitantly with a magnetic phase transition (from nonmagnetic to ferromagnetic). These results and issues have led to more investigations on the electronic, magnetic and structural properties of $Zn_{0.5}Cr_{0.5}O$.

In this paper, the electronic, magnetic and structural properties of pure and Cr-doped ZnO have been extensively investigated in LT (19 K) hexagonal wurtzite structure. It is revealed for the first time that this material encounters a nonmagnetic insulator to ferromagnetic half-metal transition for 50% Cr-doping ($Zn_{0.5}Cr_{0.5}O$). This transition is very interesting because the half-metallic ferromagnetic behavior of $Zn_{0.5}Cr_{0.5}O$ can be utilized for spintronic devices, thermochromic devices, optical and holographic devices, sensors, actuators and power meters, or thermometers. This research investigates the origin of the insulator to half-metal transition for Cr-doping in ZnO, and likewise, the origin of ferromagnetism of $Zn_{0.5}Cr_{0.5}O$.

2. Method of calculations

Self-consistent spin-polarized electronic structure calculations of pure and Cr-doped ZnO were carried out using density functional theory (DFT) (Hohenberg & Kohn, 1964; Kohn & Sham, 1965) as implemented in the tight-binding linearized-muffin-tin-orbitals (TB-LMTO) method in its atomic sphere approximations (ASA) (Anderson, 1975; Perdew & Wang, 1992). The local spin density approximations (LSDA) (Perdew & Wang, 1992; Anderson & Jepsen, 1984) were employed in the first-principles electronic structure calculations.

The ideal ZnO has a hexagonal wurtzite structure with

the space group $P6_3mc$ (space group number 186). The primitive unit cell contains two Zn and O atoms each. The Zn atom is located at the center of a tetrahedron made up of four O atoms, i.e. at the center of a ZnO_4 tetrahedron. The lattice parameters used were: $a = b = 3.2465 \text{ \AA}$ and $c = 5.2030 \text{ \AA}$, $\alpha=\beta=90^\circ$ and $\gamma=120^\circ$. Each Zn atom is located at (0.3333, 0.6667, 0.3812), whereas the O atom is located at (0.3333, 0.6667, 0) (Yoshio *et al.*, 2001). A Cr concentration of $x = 0.5$ in $Zn_{1-x}Cr_x$ was employed to investigate the substitution effect of Cr in the LT ZnO.

3. Results and discussion

3.1 Structural properties

The structure of both pure ZnO and $Zn_{0.5}Cr_{0.5}O$ in the LT phase are illustrated in Figure 1. The primitive unit cell of pure ZnO consists of two Zn and O atoms each. The Zn atoms have a four-fold coordination with O atoms. These four O atoms form a regular ZnO_4 tetrahedron with Zn at the center of such a tetrahedron (see Figure 1(a)).

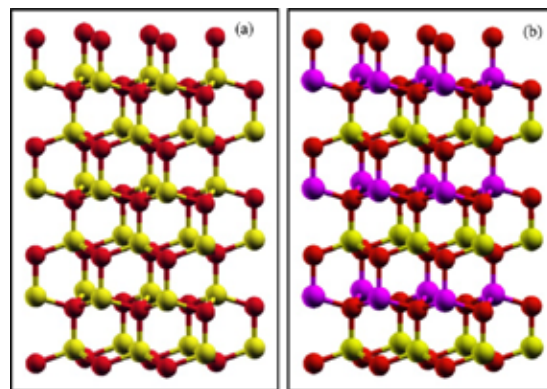


Fig. 1. Crystal structures of pure ZnO (a) and $Zn_{0.5}Cr_{0.5}O$ (b). Zn, O and Cr atoms are represented by the yellow, red and violet solid spheres

In each ZnO_4 tetrahedron, there is a single apical O atom (in the c-direction) and three basal O atoms (in the ab plane). The measured apical and basal Zn-O bond lengths are 1.9834 and 1.9737 \AA , respectively. The Zn-Zn bond distances are 3.2064 and 3.2465 \AA for apical and basal planes, respectively. The $\angle Zn-O-Zn$ angles in these two planes are 108.251° and 110.663° , respectively.

The crystal structure of $Zn_{0.5}Cr_{0.5}O$ was a point of focus. In this structure, two types of oxygen coordination are alternatively observed in the c-direction that results in the formation of alternating ZnO_4 and CrO_4 tetrahedrons running in the c-direction (Figure 1(b)). All the Zn-O, Cr-O, Zn-Zn and Cr-Cr bond lengths and $\angle Zn-O-Zn$, $\angle Cr-O-Cr$ and $\angle Zn-O-Cr$ bond angles are reported in Table 1. The apical and basal Zn-O bond lengths are shortened by 0.0023 \AA and 0.0016 \AA , respectively.

While both Zn-Zn apical and basal bond distances are reduced by 0.0029 Å, more interestingly all the $\angle\text{Zn-O-Zn}$ and $\angle\text{Cr-O-Cr}$ bond angles in the basal planes are equal (110.650°) in $\text{Zn}_{0.5}\text{Cr}_{0.5}\text{O}$. It is also noticeable from Table 1 that $\angle\text{Zn-O-Zn}$ bond angle is reduced by 0.013° . Nevertheless, the shortening of Zn-O, Zn-Zn bond distances and $\angle\text{Zn-O-Zn}$ bond angles is so small that the structural distortions of the crystal are insignificant and thus are very hard to detect experimentally.

Table 1. Calculated bond lengths and angles in ZnO and $\text{Zn}_{0.5}\text{Cr}_{0.5}\text{O}$ in hexagonal wurtzite structure at 19 K.

	ZnO		$\text{Zn}_{0.5}\text{Cr}_{0.5}\text{O}$	
	Apical	Basal	Apical	Basal
Bond lengths (Å)				
Zn-O	1.9834	1.9737×3	1.9811	1.9721×3
Cr-O	-	-	1.9811	1.9721×3
Zn-Zn	3.2064	3.2465	3.2035	3.2436
Cr-Cr	-	-	3.2035	3.2436
Bond angles ($^\circ$)				
$\langle\text{Zn-O-Zn}\rangle$	108.251	110.663×3	-	110.650×3
$\langle\text{Cr-O-Cr}\rangle$	-	-	-	110.650
$\langle\text{Zn-O-Cr}\rangle$	-	-	110.265	-

3.2 Electronic structure of pure ZnO

The formal valence of Zn in ZnO is +2 (Zn^{2+}), i.e. the number of Zn-3d electron is ten ($3d^{10}$). The hexagonal crystal field splits Zn-3d bands into triply degenerate t_{2g} and doubly degenerate e_g states. The t_{2g} states further split into $d_{3z^2-r^2}$, d_{xz} and d_{yz} orbitals, while the e_g states split into $d_{x^2-y^2}$ and d_{xy} orbitals. All the t_{2g} and e_g states are fully occupied by the available ten Zn-3d electrons. Hence, they are shifted well below E_F , resulting in the insulating behavior of ZnO. Electrons are perfectly paired in these orbitals. This result causes zero net magnetic moments. The densities of states (DOS) calculated in the LSDA method are illustrated in Figure 2. It is obvious from this figure that the DOS for both spin channels are exactly the same. The valence band is found in the energy spectrum -6.77 to 0 eV, and the conduction band is observed above 1.6 eV. Thus, the band gap detected is $E_g \sim 1.6$ eV, which is a worthy improvement over other theoretically determined values ($E_g \sim 0.73\text{-}0.76$ eV) calculated in the high-temperature structure (Osuch *et al.*, 2006; Li *et al.*, 2009).

However, these results did not affect the accuracy for

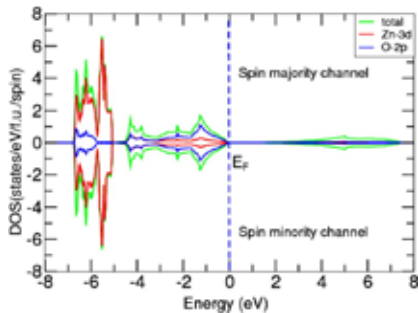


Fig. 2. Calculated total (green), Zn-3d (red) and O-2p (blue) DOS of pure ZnO at 19 K. All the Zn-3d states are fully occupied and shifted below E_F .

comparison of the related properties (e.g., band structure, DOS properties, etc.). The total DOS (TDOS), projected DOS of Zn-3d and O-2p bands are represented in Figure 2. Clearly, TDOS is predominantly due to the Zn-3d character, which is found in the energy range -6.77 to -5.09 eV, while the energy range -4.52 eV to 0 eV is O-2p dominated. The calculated DOS of Zn-3p, Zn-4s, and O-2s are also shown in Figure 3. The contributions from these levels to the TDOS are insignificant compared to the

Zn-3d or O-2p levels. Therefore, the electronic properties of ZnO depend entirely on the Zn-3d or O-2p orbitals.

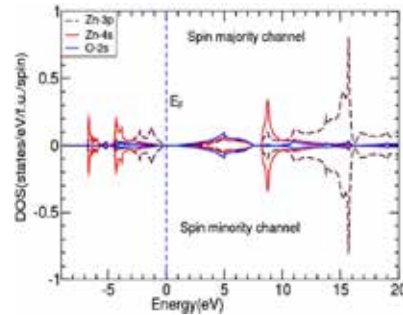


Fig. 3. Calculated DOS of Zn-3p (dotted maroon), Zn-4s (red) and O-2s (blue). The contributions to total DOS from these states are insignificant.

3.3 Electronic properties of $\text{Zn}_{0.5}\text{Cr}_{0.5}\text{O}$

Let us now concentrate on the DOS calculations of $\text{Zn}_{0.5}\text{Cr}_{0.5}\text{O}$. The primitive unit cell of $\text{Zn}_{0.5}\text{Cr}_{0.5}\text{O}$ contains one atom each of Zn and Cr and two O

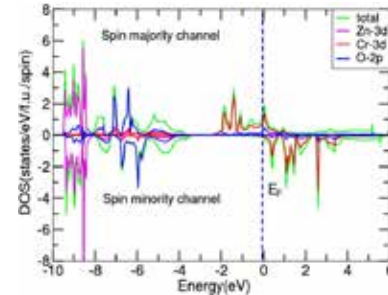


Fig. 4. Calculated total (green), Zn-3d (magenta), O-2p (blue) and Cr-3d (red) DOS of $\text{Zn}_{0.5}\text{Cr}_{0.5}\text{O}$. The system is metallic in the spin majority channel and insulating in the spin minority channel with a semiconducting energy gap ~ 3.5 eV.

atoms. Total, Zn-3d, Cr-3d and O-2p DOS are depicted in Figure 4.

For both spin channels, three groups of energy bands corresponding to Zn-3d, O-2p and Cr-3d bands are detected. In the spin-up channel, the Zn-3d $_{t_{2g}}$ and e_g bands are found around -9.5 to -8.58 eV and -8.58 to -8.15 eV, respectively. Therefore, no spin gap is observed between t_{2g} and e_g bands. Five peaks corresponding to d_{3z-r^2} , d_{xz} and d_{yz} , $d_{x^2-y^2}$ and d_{xy} states are observed at -9.4, -9.0, -8.8, -8.5 and -8.4 eV, respectively.

In the spin minority channel, Zn-3d $_{t_{2g}}$ and e_g bands are found in the energy spectrum -9.4 to 8.56 eV and -8.56 to -8.15 eV, respectively. Five peaks corresponding to d_{3z-r^2} , d_{xz} and d_{yz} , $d_{x^2-y^2}$ and d_{xy} states are respectively found at -9.36, -8.95, -8.7, -8.52 and -8.38 eV. From the calculation of the number of Zn-3d electrons and Zn-3d DOS (Table 2), it is evident that all the Zn-3d states are occupied for both spin channels. The electrons in each orbital are perfectly paired, as shown in Figure 7(a).

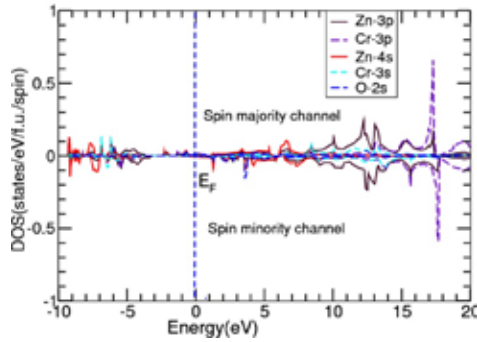


Fig. 5. Calculated Zn-3p, Zn-4s, Cr-3p, Cr-3s and O-2s DOS. Contributions to total DOS from these states are insignificant.

The formal valence of Cr in $Zn_{0.5}Cr_{0.5}O$ is +2 (Cr^{2+}). That is to say, it has four electrons in its 3d (d^4) bands. Due to strong Hund's coupling, these four electrons would occupy Cr-3d bands of majority spin channel. Out of these four electrons, three occupy t_{2g} states and the remaining single electron is shared by the e_g states. This sharing of an electron by the two e_g states is responsible for the metallic character of $Zn_{0.5}Cr_{0.5}O$. The spin minority channel remains insulating with a semiconducting gap of 3.5 eV.

Table 2. Calculated total densities of states (TDOS) and number of electrons for ZnO and $Zn_{0.5}Cr_{0.5}O$ in 19 K

	ZnO		$Zn_{0.5}Cr_{0.5}O$	
	up spin (\uparrow)	down spin (\downarrow)	up spin (\uparrow)	down spin (\downarrow)
Number of electrons				
Zn-3d	4.95	4.97	4.97	4.96
Cr-3d	-	-	3.98	0.02
DOS (states/eV/f.u./spin)				
Zn-3d	4.94	4.96	4.99	5.0
Cr-3d	-	-	3.97	0.03

Considering these two spin channels, the system is thereby a half-metal. It is also unambiguous from Figure 4 that Cr-3d $_{t_{2g}}$ and e_g bands are found in the energy windows

-2.36 to -0.87 eV and -0.87 to 1.0 eV, respectively, for the spin-up channel. The number of Cr-3d electrons calculated for the up and down spin channels is four and zero, respectively. This is consistent with the total DOS calculation at E_F (see Table 2). Furthermore, Zn-3p, 4s, Cr-3p, 3s and O-2s DOS are also calculated (Figure 5), but their contributions to the total DOS are insignificant.

To understand the electronic structure accurately, total (Figure 6(a)) and partial band structures (PBS) of all the 3d orbitals are also optimized. The PBS of d_{3z-r^2} , d_{yz} , d_{xz} , $d_{x^2-y^2}$ and d_{xy} orbitals are demonstrated in Figures 6(b) to 6(e). It is emerged out from Figures 6(b) to 6(d) that all the three t_{2g} orbitals (d_{3z-r^2} , d_{yz} and d_{xz}) are occupied by three electrons, and they are shifted below E_F . Nevertheless, the $d_{x^2-y^2}$ orbital is almost occupied, while the d_{xy} is found almost empty.

Eventually, they are still touching E_F . Therefore, the fourth electron is shared by the e_g orbital. This sharing of the single electron by the e_g orbital is responsible for the metallic nature of $Zn_{0.5}Cr_{0.5}O$ in the LT phase. The ground state magnetic moment calculated is $-3.85 \mu_B/Cr$ (Table 3) for all Cr $-ions$. This result confirms that only one kind of Cr (Cr^{2+}) is present in the crystal and consequently the Cr^{3+} -ions are absent. Therefore, any secondary phase, such as $ZnCr_2O_4$, is not observed in the structural study upon 50% Cr-doping, and there exist only CrO_4 and ZnO_4 tetrahedrons.

3.4 Magnetic properties

The undoped ZnO is found nonmagnetic, while $Zn_{0.5}Cr_{0.5}O$ is found ferromagnetic. The available ten 3d electrons are equally distributed in five Zn-3d orbitals. These are perfectly paired in the opposite direction that results in zero net magnetic moments. This is consistent with the calculated magnetic moments (see Table 3). The distribution of electrons in the t_{2g} and e_g orbitals are schematically depicted in Figure 7(a). Next, the magnetic properties of $Zn_{0.5}Cr_{0.5}O$ should be considered. The available ten Zn-3d electrons are almost equally distributed in all Zn-3d orbitals such that the effective

magnetic moment of Zn is almost zero ($-0.01\mu_B$). The effective and Cr-magnetic moments calculated are $-3.9\mu_B$ and $-3.85\mu_B$ respectively. This indicates that the effective

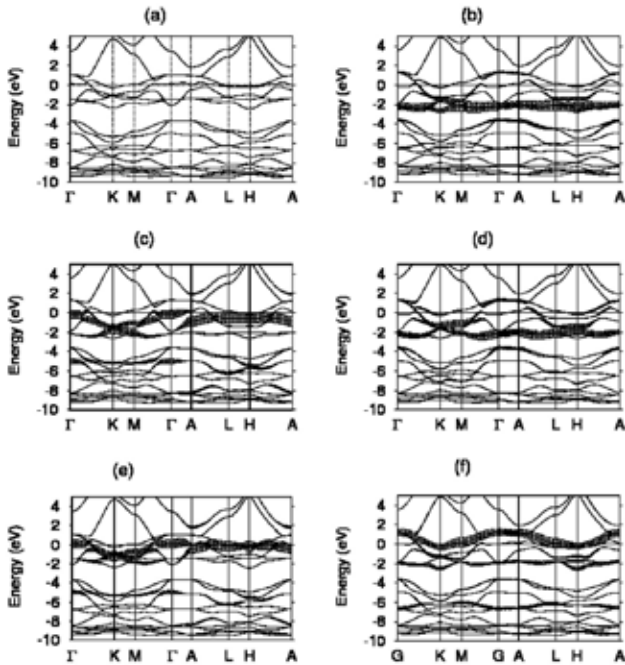


Fig. 6. Calculated partial band structures of Cr- $d_{3z^2-r^2}$ (a), d_{yz} (b), d_{xz} (c), $d_{x^2-y^2}$ (d), d_{yz} (e) and d_{xy} (f) states of $\text{Zn}_{0.5}\text{Cr}_{0.5}\text{O}$ for majority spin species. All the Cr- $d_{3z^2-r^2}$, d_{yz} , d_{xz} states are occupied. The $d_{x^2-y^2}$ state is almost occupied and d_{xy} state is almost empty but both touch the Fermi level.

Table 3. Calculated total ground state energy (eV), magnetic moments (μ_B), band gap (eV) for ZnO and $\text{Zn}_{0.5}\text{Cr}_{0.5}\text{O}$ in 19 K

	ZnO	$\text{Zn}_{0.5}\text{Cr}_{0.5}\text{O}$
Ground state energy (E_T)	-7475.68	-5986.40
Effective mag. mom. (μ_{eff})	0	-3.90
Zn - mag. mom. (μ_{Zn})	0	-0.01
Cr - mag. mom. (μ_{Cr})	-	-3.85
O - mag. mom. (μ_{O})	0	-0.04
Band gap (E_g)	1.65	0

magnetic moments arise entirely from the Cr-magnetic moments. The distributions of electrons in different orbitals are schematically depicted in Figure 7(b). All the Cr-3d electrons are aligned parallel due to the strong Hund's rule coupling. The ground state energies calculated for undoped and doped ZnO are also reported in Table 3. The ground state energy increases markedly by 1489.28 eV upon Cr-doping in ZnO. This result indicates that the repulsive force increases due to Cr-doping, meaning electron correlation predominates in the doped material $\text{Zn}_{0.5}\text{Cr}_{0.5}\text{O}$. Therefore, electron correlation together with the strong Hund's rule coupling is responsible for the ferromagnetic behavior of $\text{Zn}_{0.5}\text{Cr}_{0.5}\text{O}$.

4. Conclusions

In this work, the structural, electronic and magnetic properties are extensively studied for both pure and Cr-doped ZnO in an LT (19 K) wurtzite structure. Pure ZnO

is found to be a nonmagnetic insulator. The insulating behavior of ZnO is ascribed by the complete filling of each Zn-3d orbital and its shifting below the Fermi level. In each orbital, two electrons are perfectly paired in the opposite direction, which is responsible for the nonmagnetic behavior of pure ZnO. Interestingly, the scenario changes dramatically at 50% Cr-doping for which the material encounters an insulator to half-metal transition. This

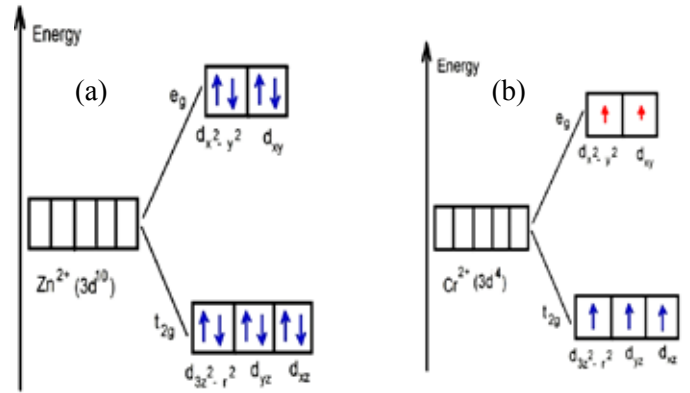


Fig. 7. The proposed distribution of electrons in different Zn-3d (1st panel) and Cr-3d (2nd panel) orbitals are schematically shown. Each blue arrow corresponds to one electron. Red arrows represent a fraction of an electron.

preserves ferromagnetism that is accompanied by strong electron correlations of Cr-3d electrons. In the spin-up channel, the system $\text{Zn}_{0.5}\text{Cr}_{0.5}\text{O}$ is found to be metallic due to the sharing of the single electron by the Cr- e_g orbitals. The electrons in the Cr-3d orbitals are identified as unpaired and aligned parallel to each other due to the strong Hund's rule coupling causing ferromagnetism. Finally, shortening of Zn-O or Zn-Zn bond distances and $\angle\text{Zn-O-Zn}$ bond angles caused by Cr-doping is insignificant for structural distortions in $\text{Zn}_{0.5}\text{Cr}_{0.5}\text{O}$.

References

- Anderson, O.K. (1975). Linear methods in band theory. *Physical Review B*, **12**(8): 3060-3083.
- Anderson, O.K. & Jepsen, O. (1984). Explicit, first-principles tight-binding theory. *Physical Review Letters*, **53**(27): 2571-2574.
- Battaglia, C., Escarre, J., So `derstro `m, K., Charriere,

- M., Despeisse, M. et al. (2011).** Nanomoulding of transparent zinc oxide electrodes for efficient light trapping in solar cells. *Nature Photonics*, **5**(9): 535-538.
- Bhargava, R., Sharma, P.K., Chawla, A. K., Kumar, S., Chandra, R., Pandey, A.C. & Kumar, N. (2011).** Variation in structural, optical and magnetic properties of $Zn_{1-x}Cr_xO$ ($x = 0.0, 0.10, 0.15,$ and 0.20) nanoparticles: Role of dopant concentration on non-saturation of magnetization. *Materials Chemistry and Physics*, **125**(3): 664-671.
- Chai G., Lupan O., Chow L. & Heinrich H. (2009).** Crossed zinc oxide nanorods for ultraviolet radiation detection. *Sensors Actuators A: Physical*, **150**(2): 184-187.
- Chen, Y., Xu, X. L., Zhang, G.H., Xue, H. & Ma, S.Y. (2010).** Blue shift of optical band gap in Er-doped ZnO thin films deposited by direct current reactive magnetron sputtering technique. *Physica E*, **42**(5): 1713-1716.
- Dietl, T., Ohno, H., Matsukura, F., Cibert, J. & Ferrand, D. (2000).** Zener model description of ferromagnetism in zinc-blende magnetic semiconductors. *Science*, **287**(5455): 1019-1022.
- Djurisi, A.B., Ng, A.M. C. & Chen, X.Y. (2010).** ZnO nanostructures for optoelectronics: Material properties and device applications. *Progress in Quantum Electronics*, **34**(4): 191-259.
- Gad, S.A., Moustafa, A.M. & Ward, A.A. (2015).** Preparation and some physical properties of $Zn_{1-x}Cr_xO$. *Journal of Inorganic and Organometallic Polymers and Materials*, **25**(5): 1077-1087.
- Gao, P.X. & Wang, Z.L. (2005).** Nanoarchitectures of semiconducting and piezoelectric zinc oxide. *Journal of Applied Physics*, **97**(4):044304(1-7).
- Gao, S., Zhang, H., Wang, X., Deng, R., Sun, D. & Zheng, G. (2006).** ZnO-based hollow microspheres: Biopolymer-assisted assemblies from ZnO nanorods. *The Journal of Physical Chemistry B*, **110**(32): 15847-15852.
- Hohenberg, P. & Kohn, W. (1964).** Inhomogeneous Electron Gas. *Physical Review*, **136** (3B): B864-B871.
- Iqbal, A., Mahmood, A., Khan, T.M. & Ahmed, E. (2013).** Structural and optical properties of Cr-doped ZnO crystalline thin films deposited by reactive electron beam evaporation technique. *Progress in Natural Science: Materials International*, **23**(1): 64-69.
- Jin, Z., Fukumura, T., Kawasaki, M., Ando, K., Saito, H et al. (2001).** High throughput fabrication of transition-metal-doped epitaxial ZnO thin films: A series of oxide-diluted magnetic semiconductors and their properties. *Applied Physics Letters*, **78**(24): 3824-3826.
- Kim, S., Nam, G., Yoon, H., Park, H., Choi, H. et al. (2014).** Structural, optical, and electrical properties of ZnO thin films deposited by sol-gel dip-coating process at low temperature. *Electronic Materials Letters*, **10**(4): 869-878.
- Kohn, W. Sham, L.J. (1965).** Self-consistent equations including exchange and correlation effects. *Physical Review B*, **140**(4A): A1133-A1138.
- Li, L., Wang, W., Liu, H., Liu, X., Song, Q. & Ren, S. (2009).** First principles calculations of electronic band structure and optical properties of Cr-doped ZnO. *The Journal of Physical Chemistry C*, **113**(19): 8460-8464.
- Lin, Y.C., Hsu, C.Y., Hung, S.K., Chang, C.H. & Wen, D.C. (2012).** The structural and optoelectronic properties of Ti-doped ZnO thin films prepared by introducing a Cr-buffer layer and post annealing. *Applied Surface Science*, **258**(4): 9891-9895.
- Osuch, K., Lombardi, E.B. & Gebicki, W. (2006).** First principles study of ferromagnetism in $Ti_{0.0625}Zn_{0.9375}O$. *Physical Review B*, **73**(7): 075202(1-5).
- Perdew, J.P. & Wang, Y. (1992).** Accurate and simple analytic representation of the electron-gas correlation energy. *Physical Review B*, **45**(23): 13244-13249.
- Rasouli, S. & Moeen, S.J. (2011).** Combustion synthesis of co-doped zinc oxide nanoparticles using mixture of citric acid-glycine fuels. *Journal Alloys and Compound*, **509**(5): 1915-1919.
- Roberts, B.K., Pakhomov, A.B., Shutthanandan, V.S. & Krishnan, K.M. (2005).** Ferromagnetic Cr-doped ZnO for spin electronics via magnetron sputtering. *Journal of Applied Physics*, **97**(10): 10D310 (1-3).
- Sato, K. & Katayama, Y.H. (2002).** First principles materials design for semiconductor spintronics. *Semiconductor Science and Technology*, **17**: 367-376.
- Shah, A.H., Ahamed, M.B., Neena, D., Mohmed, F. & Iqbal, A. (2014).** Investigations of optical, structural and antibacterial properties of Al-Cr dual-doped ZnO nanostructure. *Journal of Alloys and Compounds*: **606**: 164-170.
- Thota, S., Dutta, T. & Kumar, J. (2006).** On the sol-gel synthesis and thermal, structural, and magnetic studies of transition metal (Ni, Co, Mn) containing ZnO powders. *Journal of Physics: Condensed Matter*, **18**(8): 2473-8246.
- Ueda, K., Tabata, H. & Kawai, T. (2001).** Magnetic and electric properties of transition-metal-doped ZnO films. *Applied Physics Letters*, **79**(7): 988-990.
- Xu, C., Yang, K., Liu, Y., Huang, L., Lee, H., Chao, J. & Wang, H. (2008).** Buckling and Ferromagnetism of Aligned Cr-Doped ZnO Nanorods. *The Journal of Physical Chemistry C*, **112**(49): 19236-241.

West, K.G., Osofsky, M., Mazin, I.I., Dao, N. N.H., Wolf, A.S. & Lu, J. (2015). Magnetic properties and spin polarization of Ru doped half metallic CrO₂. *Applied Physics Letters*, **107**(1): 012402(1-4).

Yi, J., Lee, J.M. & Park, W. (2011). Vertically aligned ZnO nanorods and graphene hybrid architectures for high-sensitive flexible gas sensors. *Sensors and Actuators B: Chemical*, **155**(1): 264–269.

Yilmaz, S., Parlak, M., Ozcan, S., Altunbas, M., McGlynn, E. & Bacaksiz, E. (2011). Structural, optical and magnetic properties of Cr-doped ZnO microrods prepared by spray pyrolysis method. *Applied Surface Science*, **257**(22):9293–9298.

Yoshio, K. Onodera, A., Satop, H., Sakagami, N. & Yamashita, H. (2001). Crystal structure of ZnO:Li at 293 K and 19 K by x-ray diffraction. *Ferroelectrics*, **264**(1): 133–138.

Zheng, B.J., Lian, J.S. & Jiang, Q. (2011). Highly transparent and conductive Zn_{0.86}Cd_{0.11}In_{0.03}O thin film prepared by pulsed laser deposition. *Journal of Superconductivity and Novel Magnetism*, **24**(5): 1627–1632.

Zhuge, L.J., Wu, X.M., Chen, X.M. & Meng, Y.D (2009). Effect of defects on room-temperature ferromagnetism of Cr-doped ZnO films. *Scripta Materialia*, **60**(4): 214–217.

Zhuge, L.J., Wu, X.M., Wu, Z.F., Yang, X. M., Chen, X.M. & Chen, Q. (2010). Structure and deep ultraviolet emission of Co-doped ZnO films with Co₃O₄ nano-clusters. *Materials Chemistry and Physics*, **120**(2-3): 480–483.

Submitted :26/10/2017

Revised :27/03/2018

Acceptance :03/04/2018

دراسة عن خاصية العزل في أكسيد الزنك المخصب بالكروم مع تركيبة فورتزيت منخفض الحرارة (19 كلفن)

ساراجيت بيسواس
قسم الفيزياء، كلية تاكي الحكومية، بنغال الغربية، الهند

الملخص

تمت دراسة الخواص التركيبية والإلكترونية والمغناطيسية لأكسيد الزنك النقي والمخصب بالكروم مع تركيبة فورتزيت منخفض الحرارة (19 كلفن) من خلال استخدام نظرية الدالة الوظيفية للكثافة (DFT) كما تم تنفيذها بطريقة (TB-LMTO). وقد لوحظ أن أكسيد الزنك النقي عبارة عن عازل غير مغناطيسي، حيث وجدنا جميع مدارات Zn-3d مشغولة ووجدنا أن الإلكترونات مقترنة تماماً في كل مدار مما يجعل طبيعة أكسيد الزنك النقي غير مغناطيسية. لكن تخصيب أكسيد الزنك بالكروم قد غير خصائصه الإلكترونية والمغناطيسية بشكل كبير. فعند إحلال الكروم محل الزنك بنسبة 50% تحولت المادة من عازلة إلى مغناطيسية. وقد أوضحت هذه الدراسة أن المادة المخصبة $Zn_{0.5}Cr_{0.5}O$ هي معدنية بالنسبة لمعظم أنواع السبينات وعازلة بالنسبة للأقلية من أنواع السبينات مع فجوة شبيهة موصلة بـ 3.5 eV. نتيجة لتأثير الارتباط القوي للإلكترونات، أصبحت ثلاث مدارات $Cr-t_{2g}$ مشغولة بالكامل بثلاثة إلكترونات $Cr-3d$ ، في حين أن إلكترون وحيد متبقي يتقاسمه مداران eg في المنطقة القريبة من مستوى Fermi. هذه المشاركة في الإلكترون الوحيد بواسطة مدارين eg هي المسؤولة عن السلوك المعدني لـ $Zn_{0.5}Cr_{0.5}O$ لغالبية قنوات السبينات. وأن المحاذاة الموازية للإلكترونات غير المزدوجة في المدارات $Cr-3d$ هي المسؤولة عن المغناطيسية الحديدية لهذه المادة.